

$|\Delta E_{bs}|/|\Delta E_a|$ . For example, if asymmetric stretching gives up  $|\Delta E_a|$ , bending-symmetric stretching gains  $|\Delta E_{bs}| = G|\Delta E_a|$ . For  $G$  less than unity, translation-rotation then also gains energy; for  $G$  greater than unity it loses some to bending-symmetric stretching.

By the use of considerations from irreversible thermodynamics,<sup>4</sup> phenomenological rate equations for small departures from equilibrium can be derived:

$$de_{bs}/dt|_{\text{eq}} = (\tau_{VT})^{-1}(e_{bs}^* - e_{bs}) + (\tau_{VV})^{-1} \times [G^2(c_a/c_{bs})(e_{bs}^* - e_{bs}) - G(e_a^* - e_a)], \quad (1)$$

$$de_a/dt|_{\text{eq}} = (\tau_{VV})^{-1}[(e_a^* - e_a) - G(c_a/c_{bs})(e_{bs}^* - e_{bs})]. \quad (2)$$

The relaxation times  $\tau_{VT}$  and  $\tau_{VV}$  are for the V-T and V-V interactions, respectively;  $(e_x^* - e_x)$  is the difference between the energy per unit mass that a mode would have were it in equilibrium with translation and what it actually has;  $c_x$  is the specific heat per unit mass for the given mode. The subscript  $( )_{bs}$  refers to bending-symmetric stretching, and  $( )_a$  to asymmetric stretching. For specific cases these equations can be derived from microscopic considerations as outlined by Herzfeld and Litovitz.<sup>5</sup>

Application of the above equations to a spectrophone in which asymmetric stretching is radiatively excited gives for the phase lag  $\psi$  due to vibrational nonequilibrium

$$\tan\psi = \frac{(G + K_G - 1)\omega\tau_{VT} + [(c_{\text{tot}} - c_a)/c_{\text{tot}}]\omega\tau_{VV} + (c_{tr}/c_{\text{tot}})(1 - G)\omega\tau_{VT}^2\omega\tau_{VV}}{1 + \omega\tau_{VT}[(1 - G)K_G\omega\tau_{VT} + \{(1 - G)[(c_{\text{tot}} - c_a)/c_{\text{tot}}] - (c_{tr}/c_{\text{tot}})\}\omega\tau_{VV}]}, \quad (3)$$

where

$$K_G \equiv (c_{\text{tot}})^{-1}[G^2(c_a/c_{bs})(c_{\text{tot}} - c_a) + Gc_a + c_{\text{tot}} - c_{bs}].$$

Here,  $c_{\text{tot}}$  is the total specific heat at constant pressure;  $c_{tr}$  is the corresponding specific heat for translation-rotation. The angular frequency of modulation of the input radiation is  $\omega$ .

Work by Huetz-Aubert *et al.*<sup>6</sup> has resulted in an equation that is reproduced if  $K_G$ ,  $(c_{\text{tot}} - c_a)/c_{\text{tot}}$ , and  $c_{tr}/c_{\text{tot}}$  are here set equal to unity. The difference occurs because Huetz-Aubert *et al.* neglect certain mechanisms that contribute to the disturbances in energy of the various modes—specifically, the contributions due to collisional transfer of energy from translation-rotation to bending-symmetric stretching and also from bending-symmetric stretching to asymmetric stretching. Such mechanisms would be negligible if the above parameters were indeed unity, but unfortunately they are not. At room temperature the additional transfer of energy from translation-rotation to bending-symmetric stretching cannot be neglected.

To emphasize the importance of using a complete model accounting for all transfer mechanisms, consider Eq. (3) at room temperature and when terms of order  $(\omega\tau)^2$  and higher neglected:

$$\omega\tau_{\text{spect}} \equiv \tan\psi = (G - 0.28)\omega\tau_{VT} + \omega\tau_{VV}. \quad (4)$$

The comparable equation if  $K_G$  is set equal to unity is

$$\omega\tau_{\text{spect}} \equiv \tan\psi = G\omega\tau_{VT} + \omega\tau_{VV}. \quad (5)$$

Using Eq. (5), Huetz-Aubert *et al.* tried to ascertain which V-V transition governs  $\text{CO}_2$  relaxation. Independently obtained data were used as follows:  $\tau_{\text{spect}} = 7 \mu\text{sec}$ ,<sup>7</sup>  $\tau_{VT} = 6 \mu\text{sec}$ ,<sup>8</sup> and  $\tau_{VV} = 3.7 \mu\text{sec}$ .<sup>9</sup> These give  $G = 0.55$ , which corresponds to transitions in which two bending-mode quanta (or one symmetric stretching) are exchanged for one asymmetric-stretching quantum. Using the more complete Eq. (4), one finds  $G = 0.83$ ,

which implies the exchange of three bending-mode quanta (or one bending and one symmetric stretching) for one asymmetric-stretching quantum.

Before final conclusions about a dominant V-V transition can be made, the experimental data must be more precise; it is equally important to use theoretically complete equations to interpret the data.

\* Work supported by U.S. Air Force Office of Scientific Research under Contract F 44620-69-C-0006.

<sup>1</sup> T. L. Cottrell, I. M. MacFarlane, A. W. Read, and A. H. Young, *Trans. Faraday Soc.* **62**, 2655 (1966); T. L. Cottrell, I. M. MacFarlane, and A. W. Read, *ibid.* **63**, 2093 (1967).

<sup>2</sup> P. V. Slobadskaya, *Opt. Spektrosk.* **22**, 29, 224 (1967) [*Opt. Spectrosc.* **22**, 14, 120 (1967)].

<sup>3</sup> W. G. Vincenti, "The Use of Radiatively Driven Acoustic Waves for the Study of Vibrational Rate Processes," *Astronaut. Acta* (to be published).

<sup>4</sup> I. Prigogine, *Introduction to Thermodynamics of Irreversible Processes* (Charles C. Thomas, Springfield, Ill., 1955), pp. 14-39.

<sup>5</sup> K. F. Herzfeld and T. A. Litovitz, *Absorption and Dispersion of Ultrasonic Waves* (Academic Press Inc., New York, 1959), pp. 110-116.

<sup>6</sup> M. Huetz-Aubert, P. Chevalier, and C. Klapisz, *Compt. Rend.* **B268**, 748 (1969); M. Huetz-Aubert and P. Chevalier, *ibid.* **B268**, 965, 1068 (1969).

<sup>7</sup> See Ref. 1.

<sup>8</sup> E. H. Carnevale, C. Carey, and G. Larson, *J. Chem. Phys.* **47**, 2829 (1967).

<sup>9</sup> C. B. Moore, R. E. Wood, B. Hu, and J. T. Yardley, *J. Chem. Phys.* **46**, 4222, 4491 (1967).

## Differential Elastic Scattering of $\text{D}_2$ by $\text{N}_2$ in Crossed Molecular Beams\*

DANIEL H. WINICUR,<sup>†</sup> A. L. MOURSUND, W. R. DEVEREAUX,<sup>‡</sup> L. R. MARTIN,<sup>§</sup> AND ARON KUPPERMANN

Arthur Amos Noyes Laboratory of Chemical Physics,<sup>||</sup> California Institute of Technology, Pasadena, California 91109

(Received 22 December 1969)

Until recently, high-resolution measurements of elastic differential scattering cross sections were limited to systems containing an alkali atom because of the

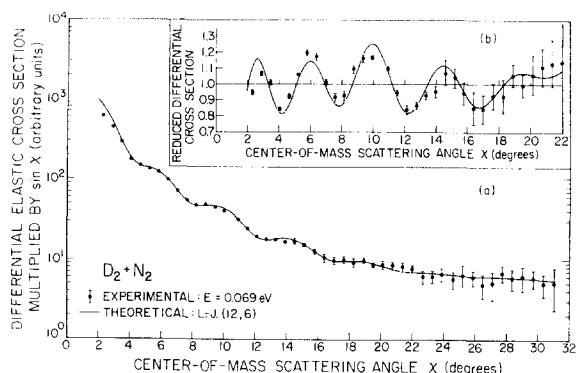


FIG. 1. (a) Center-of-mass differential elastic scattering cross section of  $D_2+N_2$  multiplied by the sine of the c.m. scattering angle at a most probable relative velocity of  $1.95 \times 10^5$  cm/sec (equivalent to 0.069 eV) vs c.m. scattering angle. The bars indicate the range of uncertainty in reading the recorder chart. The solid curve is a theoretical cross section, averaged over the relative energy spread of the beams ( $\Delta E/E=0.35$ ) and the detector width  $\Delta\chi=3$  deg, calculated for a L-J (12,6) potential with  $r_m=3.68$  Å and  $\epsilon=0.0057$  eV. (b) The differential cross sections replotted after removal of their steep angular dependences.

inherently low efficiency of electron-bombardment molecular beam detectors usually used for nonalkali systems.<sup>1,2</sup> We have measured<sup>3</sup> the nonreactive differential scattering of  $D_2$  by  $N_2$  and have observed quantum-mechanical rapid interference oscillations<sup>4</sup> from 2 to 20 deg c.m. These oscillations were visible despite the fact that the experimental cross sections are averages over the rotational quantum states, relative energy distribution, scattering volume, and detector acceptance angle. The extrema positions were fitted by a theoretical calculation assuming a spherically symmetric potential, and the position  $r_0$  of the potential zero was determined.

An early version of the apparatus has been described elsewhere.<sup>5</sup> A modulated, aerodynamically intensified (nozzle)  $D_2$  primary beam crossed an  $N_2$  nozzle beam at 90 deg. The density of the scattered  $D_2$  was measured by a differentially pumped quadrupole mass spectrometer<sup>6</sup> which was rotated about the scattering center in the plane of the two beams. The signals were integrated for up to 2 h by using a strip-chart recorder and a 100-sec lock-in amplifier time constant. The  $D_2$  and  $N_2$  beams had a full width at half-maximum (fwhm) of 0.6 and 7 deg, respectively, and the scattering volume was about 30 mm<sup>3</sup>. The width of the circular detector entrance was 1.6 deg. The Mach number<sup>7</sup> of the  $D_2$  beam, measured by a slotted-disk velocity selector, was 9; the estimated Mach number of the  $N_2$  beam was 6. The most probable relative kinetic energy  $E$  was 0.069 eV ( $1.1 \times 10^{-13}$  erg).

The points shown in Fig. 1(a) are the experimental cross sections, converted<sup>8</sup> to the c.m. coordinate system, multiplied by the sine of the c.m. scattering angle  $\chi$ . The cross sections, each divided by the value determined from a least-squares straight-line fit to a log-log plot of cross section vs  $\chi$ , are shown in Fig. 1(b). Eight extrema are clearly resolved.

The experimental results were compared with the reduced cross sections calculated by the quantum-mechanical method of partial waves using JWKB and high-energy phases at low and high  $l$ , respectively.<sup>9,10</sup> The solid curves in Fig. 1 were calculated using a Lennard-Jones (12, 6) [LJ (12, 6)] potential.<sup>11</sup> The calculated cross sections were averaged over the estimated relative energy spread  $\Delta E/E=0.35$  ( $\Delta E$  is the fwhm of an assumed triangular distribution) and over a c.m. detector width  $\Delta\chi=3$  deg.<sup>12</sup> This  $\Delta\chi$  was chosen to account for the detector acceptance angle and the finite scattering volume. The energy averaging reduced the amplitudes of the oscillations but did not significantly affect their positions. Averaging over  $\Delta\chi$  reduced the amplitudes and shifted their absolute position somewhat, but did not affect their spacing.

The spacing of the rapid oscillations is very sensitive to  $r_0$  (or  $r_m$ , the distance to the potential minimum) and relatively insensitive to the potential-energy well depth  $\epsilon$  and the potential shape.<sup>13</sup> Values for  $r_0$  obtained from the extrema spacing for three spherically symmetric potentials are:  $3.08 \text{ Å} \pm 5\%$  ( $r_m=4.10 \text{ Å}$ ) for a "soft" potential [compound LJ (4, 12; 120, 6)]<sup>13,14</sup>;  $3.28 \text{ Å} \pm 5\%$  ( $r_m=3.68 \text{ Å}$ ) for a LJ (12, 6);  $3.32 \text{ Å} \pm 5\%$  ( $r_m=3.58 \text{ Å}$ ) for a "hard" potential [LJ (24, 6)]. The value obtained for  $\epsilon$  for all three potentials is 0.0057 eV ( $0.92 \times 10^{-14}$  erg)  $\pm 50\%$ . The limits reflect the experimental uncertainty in the extrema positions and the sensitivity of the extrema spacing to the potential parameters, but ignore a 5% uncertainty in the relative velocity and possible effects of asymmetry.

We gratefully acknowledge invaluable contributions made by O. H. Crawford, J. B. Cross, and Y. Kaneko, in the design, construction, and testing of the apparatus and many helpful discussions with D. G. Truhlar and R. K. B. Helbing. We are indebted to R. B. Bernstein for pointing out an error in the lab to c.m. transformation used in our original manuscript and in Ref. 3.

\* Work supported in part by the U.S. Atomic Energy Commission. Report Code No. CALT-767P4-57.

† Shell Companies Foundation Fellow.

‡ National Science Foundation Graduate Fellow.

§ Present address: Department of Chemistry, University of California, Riverside, Calif. 92502.

|| Contribution No. 3996.

<sup>1</sup> See H. Pauly and J. P. Toennies, *Methods Exptl. Phys.* **7**, 227 (1968), Pt. A.

<sup>2</sup> (a) Low-angle differential cross sections for Ar and Ne have been measured by J. Penta, C. R. Mueller, W. Williams, R. Olson, and P. Chakraborti, *Phys. Letters* **25A**, 658 (1967); W. Williams, C. R. Mueller, P. McGuire, and B. Smith, *Phys. Rev. Letters* **22**, 121 (1969). (b) The differential scattering of metastable He by He and Ar has been measured by J. Grosser and H. Haberland, *Phys. Letters* **27A**, 634 (1968); rapid oscillations have been observed for metastable He+Ar [J. Grosser and H. Haberland (private communication)]. (c) A rainbow maximum has been resolved in the scattering of Ar by  $N_2$  by R. W. Bickes, Jr. and R. B. Bernstein, *Chem. Phys. Letters* **4**, 111 (1969).

<sup>3</sup> A preliminary measurement was reported by D. H. Winicur, L. R. Martin, A. L. Moursund, W. R. Devereaux, and A. Kuppermann, *Proc. Intern. Conf. Phys. Electron. At. Collisions* 6th MIT, 1969, 185 (1969).

<sup>4</sup> See R. B. Bernstein, *Advan. Chem. Phys.* **10**, 75 (1966).

<sup>5</sup> O. H. Crawford, Ph.D. thesis, University of Illinois, 1966; J. B. Cross, Ph.D. thesis, University of Illinois, 1966.

<sup>6</sup> Extranuclear Laboratories, Inc., P. O. Box 11512, Pittsburgh, Pa. 15238, Model QPS.

<sup>7</sup> See J. B. Anderson, R. P. Andres, and J. B. Fenn, *Advan. Chem. Phys.* **10**, 275 (1966).

<sup>8</sup> F. A. Morse and R. B. Bernstein, *J. Chem. Phys.* **37**, 2019 (1962).

<sup>9</sup> Significant contributions to the development of these computer programs were made by U. Buck, R. Feltgen, and R. K. B. Helbing.

<sup>10</sup> A test calculation using exact phase shifts confirmed that the JWKB approximation introduced a negligible error.

<sup>11</sup> The quantum calculation shows no rainbow maximum; the classical rainbow angle is at about 10 deg c.m.

<sup>12</sup> Test calculations showed that the effect of averaging over  $\Delta x$  instead of a laboratory detector width was negligible.

<sup>13</sup> U. Buck and H. Pauly, *Z. Physik* **208**, 390 (1968).

<sup>14</sup> This potential form roughly approximates the "soft" potential found by U. Buck and H. Pauly, *J. Chem. Phys.* **51**, 1662 (1969).

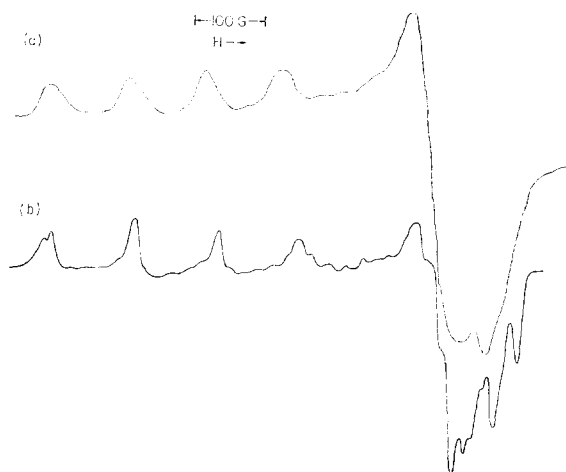


FIG. 1. (a) Room temperature ESR powder spectrum of copper-doped strontium tartrate at 9.285 GHz. (b) The same sample at 100°K.

## Notes

### Electron Spin Resonance Study of Transition Elements in Strontium Tartrate and Calcium Tartrate\*

JOSEPH BOHANDY AND JOHN C. MURPHY

*Applied Physics Laboratory, The Johns Hopkins University, Silver Spring, Maryland 20910*

(Received 14 October 1969)

We have observed the electron spin resonance (ESR) spectra of several transition element ions in single crystals of calcium tartrate tetrahydrate (CaTr) and strontium tartrate tetrahydrate (SrTr). The crystals are grown in silica gel<sup>1</sup> with a few percent of the dopant apparently entering substitutionally. The crystals are orthorhombic and have the  $P2_12_12_1$  space group with four nonequivalent molecules per unit cell.<sup>2,3</sup> Room temperature ESR spectra of single crystals of CaTr:Cu showed many similarities to the SrTr:Cu system.<sup>4</sup> Four nonequivalent sites for the  $\text{Cu}^{2+}$  ion and the same symmetry directions and planes were present. To bypass the multiple site problem, the spin-Hamiltonian parameters were obtained from powder spectra. The lines of an ESR powder spectrum usually give directly the components of the  $g$  tensor and the hyperfine splitting

(hfs) tensor.<sup>5</sup> X-band ESR powder spectra of SrTr:Cu at 300 and 100°K are shown in Figs. 1(a) and 1(b), respectively.  $\text{Cu}^{2+}$  hfs is observable along all principal axes in the better resolved 100°K spectrum. The  $^{63}\text{Cu}$  and  $^{65}\text{Cu}$  isotope splitting is also resolved. Comparison of this spectrum with a KU-band powder spectrum at 100°K clearly distinguished between  $g$  value and hfs contributions to the overlapping lines and allowed the determination of all the spin-Hamiltonian parameters. The results for CaTr:Cu and SrTr:Cu are listed in Table I.

In both systems,  $g_{zz}$  decreases and  $A_{zz}$  increases with decreasing temperature; however, there is little change below 100°K. Furthermore, there is a second  $\text{Cu}^{2+}$  resonance with slightly different temperature-independent hfs splittings in CaTr. Dehydration effects indicate that the  $\text{Cu}^{2+}$  hfs may depend on the number of  $\text{H}_2\text{O}$  molecules near the ion. No similar "second" resonance was observed in the SrTr:Cu system. Evidence for an additional  $z$  direction was also observed in the CaTr:Mn system by Wakim.<sup>6</sup>

The ESR spectrum of SrTr:Mn consists of 120 main lines plus "forbidden" transitions, the expected result for  $\text{Mn}^{2+}$  ( $S = \frac{5}{2}$ ,  $I = \frac{5}{2}$ ) ions in four nonequivalent sites. The symmetry planes and axes are the same as in SrTr:Cu. The angles which the  $z$  component of the  $g$  tensor makes with the crystallographic axes are essentially the same as those found by Wakim *et al.* for CaTr:Mn.<sup>6</sup> The parameters of the spin Hamiltonian containing the cubic fourth-order spin terms were obtained from a least-squares fit of the data using a computer program written by Swalen and Gladney<sup>7</sup> and are listed in Table I. The large uncertainty in  $E$  is due to the uncertainty in the Euler angle,  $\psi$ , which could not be determined accurately due to the multiple sites.

Preliminary studies of SrTr:Ni, SrTr:V, and SrTr:Co were also made. ESR lines due to  $\text{Ni}^{2+}$  were not observed, even at 4.2°K, presumably due to a very large

TABLE I. Spin-Hamiltonian parameters of SrTr:Cu, CaTr:Cu, and SrTr:Mn.

SrTr:Cu	CaTr:Cu	SrTr:Mn
$g_{xx} = 2.115 \pm 0.002$	$2.061 \pm 0.002$	$g = 2.002 \pm 0.002$
$g_{yy} = 2.052 \pm 0.002$	$2.111 \pm 0.002$	$D = 528 \text{ G} \pm 2 \text{ G}$
$g_{zz} = 2.393 \pm 0.001$	$2.406 \pm 0.001$	$E = 83 \text{ G} \pm 20 \text{ G}$
$A_{xx} = 18 \text{ G} \pm 2 \text{ G}$	$23 \text{ G} \pm 2 \text{ G}$	$a = 5 \text{ G} \pm 1 \text{ G}$
$A_{yy} = 27 \text{ G} \pm 2 \text{ G}$	$21 \text{ G} \pm 2 \text{ G}$	$A_{zz} = -102 \text{ G} \pm 1 \text{ G}$
$A_{zz} = 109 \text{ G} \pm 1 \text{ G}$	$107 \text{ G} \pm 1 \text{ G}$	$A_{xx} = A_{yy} = -94 \text{ G} \pm 1 \text{ G}$